International Journal of Civil Engineering

Soil Mechanics Classic

A generalized plasticity constitutive model for sand-gravel mixtures

Mehdi Goorani[1], Amir Hamidi[2,*]

Received: December 2014, Revised: May 2015, Accepted: June 2015

Abstract

This paper presents a model for prediction of the mechanical behavior of sand-gravel mixtures using generalized plasticity and critical state concepts. Proposed model is based on the difference between critical state lines of sand and sand-gravel mixture in e-Lnp' plane. A generalized plasticity model is considered as the base model for sandy soil. Its state parameter, dilation rate and hardening function are modified to involve the effects of gravel particles on the behavior of mixture. Gravel content is considered as a physical parameter for determination of four new added parameters of the model. Verification of the proposed model performed considering four sets of experiments conducted by different researchers on poorly graded sand-gravel mixtures. According to the results, proposed model provides satisfactory qualitative and quantitative predictions of the behavior of sand-gravel mixture. Stress- strain behavior besides volumetric strains in drained condition and induced pore pressure during undrained loading are satisfactory predicted which indicates the possibility of its application in boundary value problems of geotechnical engineering.

Keywords: *Constitutive modeling, Sand-gravel mixture, Generalized plasticity, Critical state, Deviatoric stress, Volume change.*

1. Introduction

Composite sand-gravel mixtures are widely used as borrow materials in construction of the earth and rockfill dams, trenches and backfills, filtering and drainage and many other civil engineering activities. In recent years, several experimental studies have been performed to investigate the mechanical behavior of sand-gravel mixtures.

Concept of far-field matrix density was first introduced to consider the effects of oversize particles on the density, static strength and deformation behavior of sand-gravel mixtures [1]. According to this criterion, the matrix is divided into two components that are the matrix immediately adjacent to the oversize particles, called near-field matrix and the material further away from the oversize particles, called far-field matrix. It was determined that the static strength and deformation behavior of granular soils with oversized particles are governed by the far-field matrix density when the oversized particles are floated in a finer-grained matrix. Also it was showed that the presence of oversized particles decreases the far-field matrix density.

A number of researchers investigated dynamic behavior of sand-gravel mixtures besides liquefaction and cyclic resistance of these soils [2-5] and concluded that increase in gravel content influences the cyclic resistance of the mixture.

Direct shear test has been used to investigate the effect of gravel particle size on the mechanical behavior of poorly graded sand-gravel mixtures [6]. It has been concluded that increase in gravel size increases the shear strength and ultimate dilation of the sand-gravel composite. Effect of gravel content on sandy matrix was also considered and it was concluded that the behavior is controlled by sand matrix in low gravel contents and by gravel particles in higher gravel contents [7]. Static triaxial tests besides dynamic torsional shear tests have also been performed to consider the mechanical behavior of poorly graded sand-gravel mixtures in a wide range of densities at the undrained condition [8]. Moreover, large scale consolidated undrained triaxial shear tests have been used to evaluate critical state characteristics of well graded gravely sands [9].

Large scale direct shear tests have been conducted to evaluate Bolton's shear strength-dilation relation [10] for sand-gravel mixtures. Based on the results, governing equations were modified using minimum void ratios of the sand and sand-gravel mixture and new formulations were presented to illustrate shear strength-dilation relation in sand-gravel composite [11].

Other researchers used triaxial tests to investigate the stiffness and shear strength characteristics of sand-gravel mixtures [12-14]. Large scale direct shear tests were also

** Corresponding author: hamidi@khu.ac.ir*
1 Graduate Student, Kharazmi University, Tehran, Iran
2 Associate Professor, School of Engineering, Kharazmi University, P.O.Box 15614, Tehran, Iran

[DOI: 10.22068/IJCE.13.2.133]

applied to investigate the mechanical behavior of sand-gravel mixtures considering different parameters like relative density, gravel content, gradation, gravel shape, gravel size and surcharge pressure [15-18]. They also evaluated the ability of Bolton's shear strength-dilation relations for sand-gravel mixtures and performed some modifications considering the effects of particle breakage in high surcharge pressures. Based on the results, increase in gravel content resulted in the increase of shear strength and ultimate dilation of the mixture. In addition, increase in gravel content increased brittleness and initial stiffness of sand-gravel mixture. A number of other researchers have investigated the mechanical behavior of coarse grained granular and rockfill materials [19-22].

Most of the previous constitutive models have been developed considering the behavior of sandy matrix without paying attention to the effects of the gravel particles on the mechanical behavior of the mixture. Considering energy equilibrium equations and particle breakage effects, mechanical behavior of coarse grained basalt was investigated [23]. A constitutive model has also been suggested considering the role of anisotropy for the coarse-grained gravely soils [24]. Other researchers have presented constitutive models for crushable granular materials [25]. Others also suggested three dimensional bounding surface plasticity models for the soil at the earth dam shells [26].

The generalized plasticity (GP) theory was first introduced by Zienkiewicz and Mroz [27] and later extended by Pastor et al. [28] for various soil types. The main advantage of GP models lie in their capability of simulating strain-stress response in different initial conditions under monotonic and cyclic loading without need of an explicit definition of yield or plastic potential surface. However, some limitations of the original models restrict their wide application. Therefore, based on GP theory, many researchers have proposed various enhanced models to improve the capability of the original model. Ling and Liu [29] proposed a GP model considering pressure dependency and densification behavior of sands. Also Ling and Yang [30] introduced the first critical state GP model. In recent years, more attention has been paid to unsaturated geomaterials. Santaguliana and Schrefler [31] suggested a GP constitutive model for unsaturated soils. Lashkari and Latifi [32] proposed a GP model for liquefaction of sands under continuous rotation of principal stress axes. Some GP models have also been introduced for soil structure interaction problems, for example Liu and Ling [33] and Lashkari [34]. More recently, GP models have been adopted for soft rocks like sandstone by Weng and Ling [35]. In present study, a recent version of the GP constitutive models presented by Manzanal et al. [36] is modified to simulate the mechanical behavior of poorly graded sand-gravel mixtures. State parameter, dilation rate and hardening modulus have been modified considering gravel content as a key parameter to model the behavior in a wide range of confining stresses and relative densities. The main objective is constitutive modeling of the behavior of sand-gravel mixture in gravel contents lower than phase transformation point, where the oversized grains are floated in finer matrix and the behavior is controlled by both sand and gravel phases.

2. The Base Model for Sand

Manzanal et al. [36] GP model which is an expanded form of Pastor et al. [28] model is considered as the base model for sand. Manzanal et al. presented the model based on the state parameter concept introduced by Been and Jefferies [37] considering the following aspects: (1) the dependency of dilatancy expression on density and confining pressure, (2) the relation between maximum mobilized friction angle (or maximum stress ratio) and softening behavior and its dependency on the initial state of soil, (3) the flow rule associated with state parameters existing in an explicit or implicit form, and (4) dependency of the isotropic plastic modulus on density variations. Concerning these issues, state parameter has been imbedded in both flow rules and formulations of plastic modulus.

In this model, projection of critical state line in *e-p'* space is considered according to the following equation originally suggested by Li and Wang [38]:

$$e_{cs} = e_{\Gamma} - \lambda\left(\frac{p'_{cs}}{p_a}\right)^{\zeta_c} \tag{1}$$

e_{Γ} is the void ratio in mean effective stress of zero, λ is the slope of critical state line in $e-(p'/p_a)^{\zeta_c}$ space, p'_{cs} and e_{cs} indicate mean effective stress and void ratio in critical state, p_a is the atmospheric pressure and ζ_c is a parameter.

State parameter (ψ) can then be determined as follows. In this equation *e* is the void ratio in each stage of loading.

$$\psi = e - e_{cs} \tag{2}$$

Elastic modulus can also be calculated based on the following equations:

$$K = K_{ev0}\, p_a \frac{(2.17-e)^2}{(1+e)}\sqrt{\frac{p'}{p_a}} \tag{3}$$

$$G = G_{es0}\, p_a \frac{(2.17-e)^2}{(1+e)}\sqrt{\frac{p'}{p_a}} \tag{4}$$

In this equation *p'* is the mean effective stress at each point of the stress path, K_{ev0} and G_{es0} are non- dimensional parameters of the constitutive model. Also $\mathbf{n}_\mathbf{g}^\mathbf{T}$ is the normal vector of potential surface and can be evaluated by the following relation:

$$\mathbf{n}_\mathbf{g}^\mathbf{T} = \frac{1}{\sqrt{1+d_g^2}}\left(d_g, 1\right) \tag{5}$$

[DOI: 10.22068/IJCE.13.2.133]

Here, d_g is the rate of dilation and is defined as follows:

$$d_g = \frac{d_0}{M_g} \cdot \left(M_g \cdot \exp(m\psi) - \eta\right) \quad (6)$$

d_0 and m are model parameters. Also M_g is the slope of the critical state line in $q - p'$ plane and η is the stress ratio in each stage of loading. Furthermore, $\mathbf{n}^T$ defines yield direction and can be determined based on the following equation:

$$\mathbf{n}^T = \frac{1}{\sqrt{1+d_f^2}}\left(d_f, 1\right) \quad (7)$$

Where d_f is a model parameter which can be estimated as follows:

$$d_f = \frac{d_0}{M_f}(M_f . \exp(m\psi) - \eta) \quad (8)$$

The proposed relation between M_f and M_g is as follows:

$$\frac{M_f}{M_g} = h_1 - h_2 \cdot \left(\frac{e}{e_{cs}}\right)^{\beta} \quad (9)$$

Here, h_1, h_2 and β are model parameters. The following equation has been suggested for plastic moduli H_L [36]:

$$H_L = H_0 \cdot \sqrt{p \cdot p_a} \cdot H_{DM} \cdot f(\eta;\psi) \quad (10)$$

H_{DM} is a function that incorporates material memory in a simple manner.

$$f(\eta;\psi) = 1 \quad \text{for } \eta = 0 \quad (11)$$

$$f(\eta;\psi) = H_f \cdot (H_v + H_s) \quad \text{for } \eta \neq 0 \quad (12)$$

H_0 is defined based on the following equation:

$$H_0 = H_0' \cdot \exp\left[-\beta_0' \cdot (e/e_{cs})^{\beta}\right] \quad (13)$$

H_0' and β_0' are model parameters and H_f can be determined based on the following equations:

$$H_f = \left(1 - \frac{\eta}{\eta_f}\right)^4 \quad (14)$$

$$\eta_f = \left(1 + \frac{1}{\alpha}\right) M_f \quad (15)$$

α is a model parameter. Also H_v and H_s can be found as follows:

$$H_v = H_{v0} \cdot \left[M_g \cdot \exp(-\beta_v \cdot \psi) - \eta\right] \quad (16)$$

$$H_s = \beta_1 . \exp(-\beta_0 . \xi_{dev}) \quad (17)$$

H_{v0} and β_v are also model parameters and β_0 and β_1 can be considered as zero for saturated condition. Finally ξ_{dev} is the accumulated deviatoric plastic strain. The relation of stress and strain rates can be utilized based on the following equation in generalized plasticity theory:

$$\dot{\boldsymbol{\sigma}} = \mathbf{D}^{ep}\dot{\boldsymbol{\varepsilon}} \quad (18)$$

In this equation, $\dot{\boldsymbol{\sigma}}$ is the rate of stress, $\dot{\boldsymbol{\varepsilon}}$ is the rate of strain and $\mathbf{D}^{ep}$ is the elasto-plastic constitutive matrix which is defined as follows:

$$\mathbf{D}^{ep} = \mathbf{D}^{\mathbf{e}} - \frac{\mathbf{D}^{\mathbf{e}}\mathbf{n}_{\mathbf{g}}\mathbf{n}^{\mathbf{T}}\mathbf{D}^{\mathbf{e}}}{H_L + \mathbf{n}^{\mathbf{T}}\mathbf{D}^{\mathbf{e}}\mathbf{n}_{\mathbf{g}}} \quad (19)$$

Where, $\mathbf{D}^e$ is the elastic constitutive matrix and H_L is the plastic modulus. As it can be seen, Manzanal et al. model [36] is based on 16 parameters for saturated condition. In the following sections, the base model is modified for sand-gravel mixture by introducing 4 new parameters.

3. Modification of the Base Model for Sand-Gravel Mixture

State parameter, dilation rate and hardening modulus of the base model are modified to model the behavior of sand-gravel mixtures.

3.1. Modification of the state parameter

According to previous studies, addition of gravel particles to a sandy host changes its behavior to a more dilative one [15]. As a result, critical state line of sand-gravel mixture in *e-Lnp*' plane moves above that of pure sand. In this regard, Eq. (2) is modified by addition of Δe based on the following equations:

$$\psi = e - e_{cs} + \Delta e \quad (20)$$

Δe can be interpreted based on the gravel content using the following relation:

$$\Delta e = r(GC)^z \quad (21)$$

Here, z is a new parameter as a function of the gravel content (GC) in the mixture. Also r is another model parameter which can be determined based on gravel content and initial mean effective stress, P_0' (kPa) by the following relations:

[DOI: 10.22068/IJCE.13.2.133]

$$z = 0.001(GC) - 0.003 \quad (22)$$

$$r = -0.0002P_0' + 0.04(GC)^{0.47} \quad (23)$$

Figure (1) shows the variation of parameter *z* with gravel content for different sets of experimental data. As it can be seen, a linear regression can be used to estimate *z* based on *GC*. Figure (2) also displays variation of parameter *r* with both initial confining pressure and gravel content for the same sets of experimental data. Regression curves for Eq. (27) is also included in this figure.

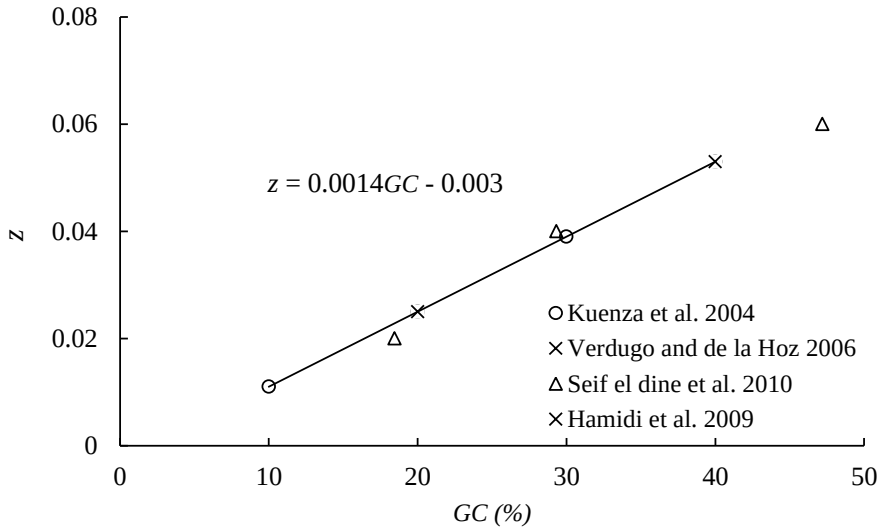

Fig. 1 Regression process on different sets of experimental data for determination of parameter *z*

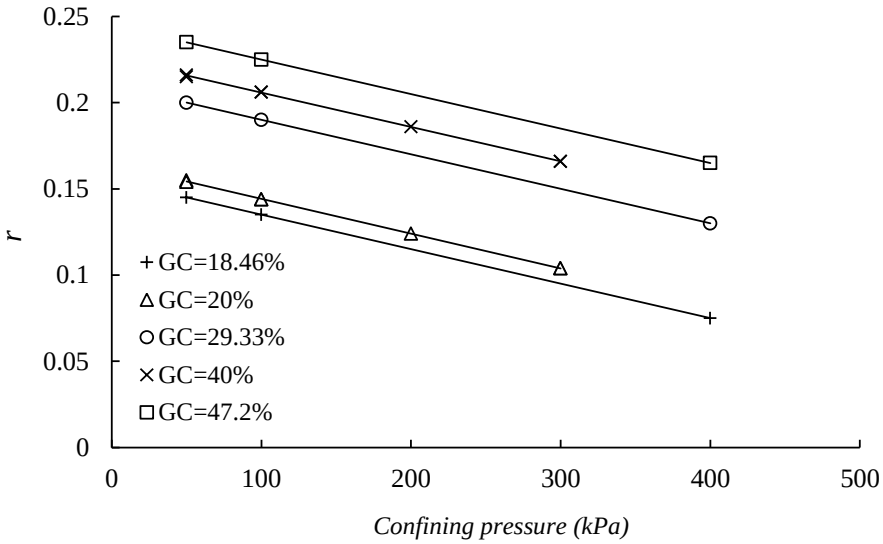

Fig. 2 Regression process on different sets of experimental data for determination of parameter *r*

3.2. Modification of dilation rate

Equations (6) and (8) of the base model are modified here for sand-gravel mixture by defining a new model parameter, *d*:

$$d_g = \frac{d}{M_g}(M_g.\exp(m\psi) - \eta) \quad (24)$$

$$d_f = \frac{d}{M_f}(M_f.\exp(m\psi) - \eta) \quad (25)$$

Where, *d* can be defined as follows based on gravel content:

$$d = d_0 \exp[s(GC)] \quad (26)$$

s is a model parameter which can be determined based on calibration with experimental data. Also, other parameter h_2 in Eq. (9) is modified based on the following relation:

$$h_2 = 0.8 + b(GC) \quad (27)$$

Here, *b* is another parameter which can be considered about 0.02 for drained and undrained conditions.

[DOI: 10.22068/IJCE.13.2.133]

3.3. Modification of the hardening modulus

Equation (11) for the hardening modulus of the base model is also modified for sand-gravel mixture based on gravel content as follows:

$$H_0 = H'.\exp[-\beta'_0.(e/e_{cs})^{\beta}] \quad (28)$$

Here, H' can be defined as follows:

$$H' = H'_0.\exp[a(GC)] \quad (29)$$

Where, a is another model parameter which can be found based on model calibration.

4. Parameters of Model

The modified model is based on four additional parameters; i.e. r, z, s and a. These parameters have been defined to consider the effects of gravel particles on the mechanical behavior of sandy soil.

Two first parameters r and z influence the state parameter of the model. Increase in each one increases the magnitude of the critical state void ratio. The process of regression for determination of these two parameters was previously depicted in Figs. (1) & (2) based on gravel content and initial confinement values.

Parameter s affects dilation rate and the other parameter a, influences the hardening modulus. Increase in its value changes the strain hardening behavior to a strain softening one. These two parameters cannot directly be computed using gravel content or confining pressure as like as parameters r and z. However, they can be determined during the process of model training and calibration using experimental data. Parameter s can also be obtained by justification of the model and experimental results for flow rule or variation of the plastic volumetric strains to plastic shear strains against the stress ratio in different gravel contents. The other parameter a, can be obtained by justification of the model and testing data for variations of the hardening modulus in different gravel contents.

In order to investigate the effect of each parameter on the behavior of sand-gravel mixture, results of triaxial compression tests on sandy soil mixed with 20% volume content (29.33% weight content) gravel particles are considered [14]. Figures (3) and (4) show the variation of deviatoric stress and volumetric strain with axial strain by the change in each model parameter, respectively. It can be concluded that the shear strength and dilative behavior of sand-gravel mixture decreases with increase in parameters r and z. Shear strength value is not too much sensitive to variations in parameter s, however, volumetric strain increases with it. Finally, increase in parameter a increases shear strength and dilative volumetric strains.

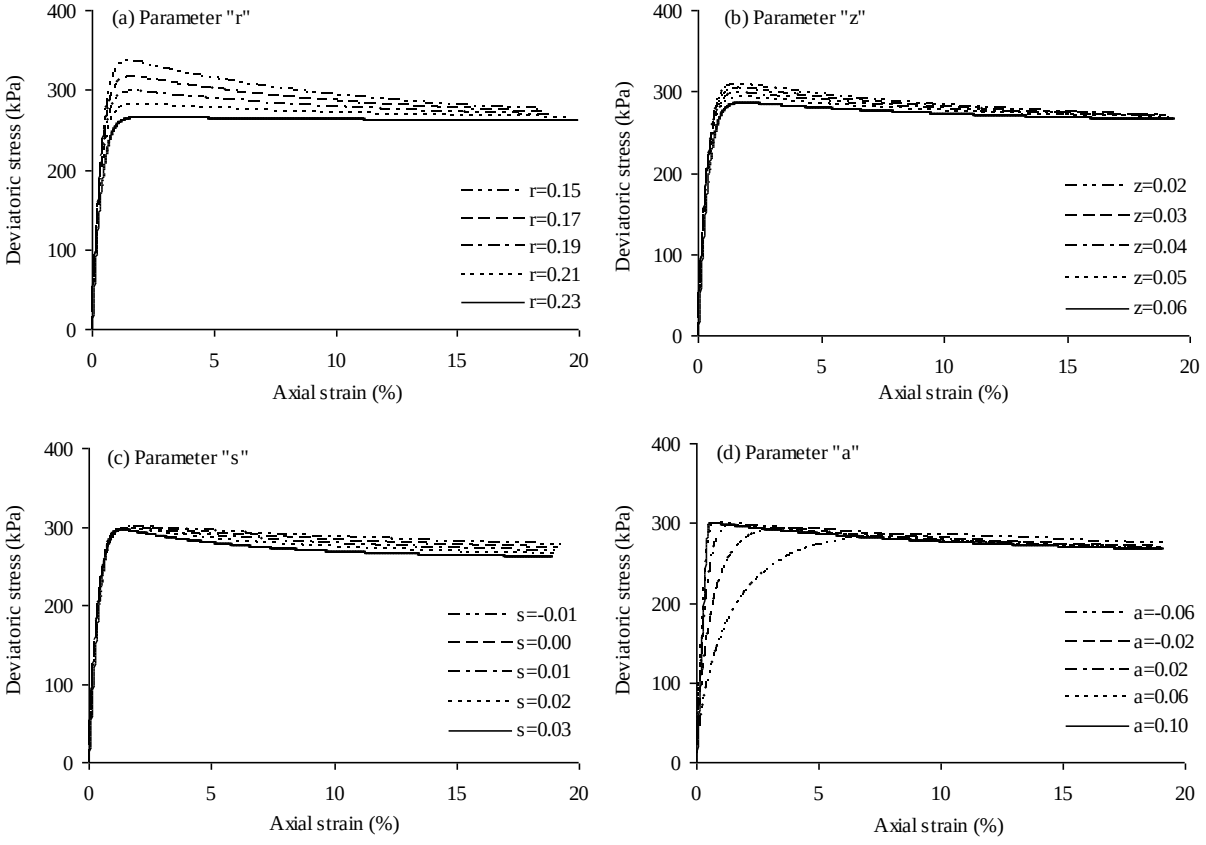

Fig. 3 Sensitivity analysis for deviatoric stress-axial strain curves (p'_0=100 kPa, Dr=70%, GC=29.33%) (a) Parameter r (b) Parameter z (c) Parameter s (d) Parameter a

[DOI: 10.22068/IJCE.13.2.133]

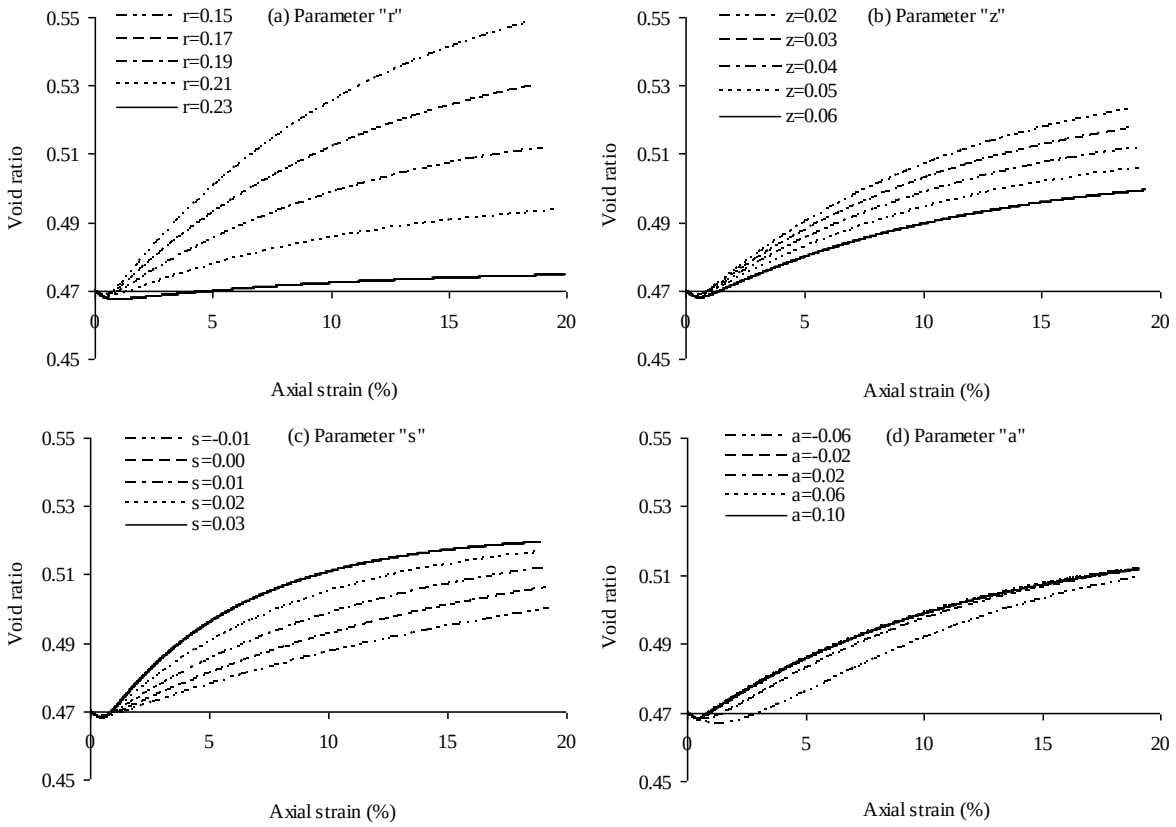

Fig. 4 Sensitivity analysis for void ratio-axial strain curves (p'_0=100 kPa, Dr=70%, GC=29.33%) (a) Parameter *r* (b) Parameter *z* (c) Parameter *s* (d) Parameter *a*

5. Verification of the Model

Four different sets of experimental data are considered to investigate the model abilities and verification of its performance [8, 13-15].

5.1. Model verification for Kuenza et al. [8] experimental data

The tests have been performed on Yurakucho sand mixed with different gravel contents in a constant mean effective stress of 49 kPa and relative densities of 30, 47 and 60 percent using hollow cylinder torsional shear apparatus in consolidated undrained condition. Physical parameters of tested soil are listed in Table (1).

Table 1 Physical parameters of the considered sandy soils in model verification

Soil type	Mean diameter,	Uniformity coefficient,	Curvature coefficient,	Minimum void ratio,	Maximum void ratio,	Specific gravity,	Minimum dry density,	Maximum dry density,
	D_{50}	C_u	C_c	$e_{\min}$	$e_{\max}$	G_s	$\rho_{d,\min}$	$\rho_{d,\max}$
Fontainebleau sand [8]	0.21	1.52	---	0.54	0.94	2.65	1.37	1.72
Chilean rivers sand [13]	0.23	11.0	---	---	---	2.63	1.52	2.04
Yurakucho sand [14]	0.22	2.51	0.83	0.74	1.24	2.69	---	---
Babolsar sand [15]	---	1.75	---	0.58	0.98	2.74	---	---

Parameters of Manzanal et al. [36] base model for Yurakucho sand are listed in Table (2). Table (3) indicates additional model parameters for the modified model which are determined based on gravel content, initial mean effective stress and calibration for the experimental data. Test results for the relative density of 60% are used in model training and calibration of the parameters. Then, the model is tested for relative densities of 30% and 47%.

[DOI: 10.22068/IJCE.13.2.133]

Table 2 Base model parameters for different sets of experimental data

Parameter		Yurakucho Sand [8]	Chilean rivers sand [13]	Fontainebleau Sand [14]	Babolsar Sand [15]
Elasticity	K_{ev0}	200	210	290	275
	G_{es0}	125	140	135	140
Critical state	M_g	0.92	1.6	1.33	1.8
	e_Γ	0.95	0.55	0.8	0.8
	λ	0.02	0.03	0.04	0.02
	ζ_c	0.7	0.4	0.6	0.5
Plastic Flow	d_0	0.6	1.6	0.7	0.7
	m	0.5	5.0	0.5	2.0
	h_1	1.3	1.6	1.5	1.6
	h_2	0.8	0.8	0.8	0.8
	α	0.45	0.45	0.45	0.45
Plastic modulus	H_0'	125	28	135	100
	β_0'	3.2	1.5	2.2	1.0
	β	1.8	0.6	0.6	0.4
	H_{v0}	100	135	100	100
	β_v	1.5	3.0	1.5	2.0

Table 3 Additional parameters for sand-gravel mixture in experimental studies of Kuenza et al. [8]

GC (%)	$s^{(1)}$	$a^{(1)}$	$z^{(2)}$	$r^{(3)}$
10	0.04	0.03	0.011	0.11 (p'_0=49 kPa)
20	0.03	0.03	0.025	0.155 (p'_0=49 kPa)
30	0.025	0.03	0.039	0.205 (p'_0=49 kPa)
40	0.02	0.03	0.053	0.215 (p'_0=49 kPa)

[1] Calculated from calibration.

[2] Calculated from equation (22).

[3] Calculated from equation (23).

Figure (5) shows deviatoric stress-axial strain curves and Fig. (6) indicates deviatoric stress-mean effective stress curves for sand-gravel mixture in different relative densities. According to these figures, fairly good agreement can be observed between experimental data and model results.

[DOI: 10.22068/IJCE.13.2.133]

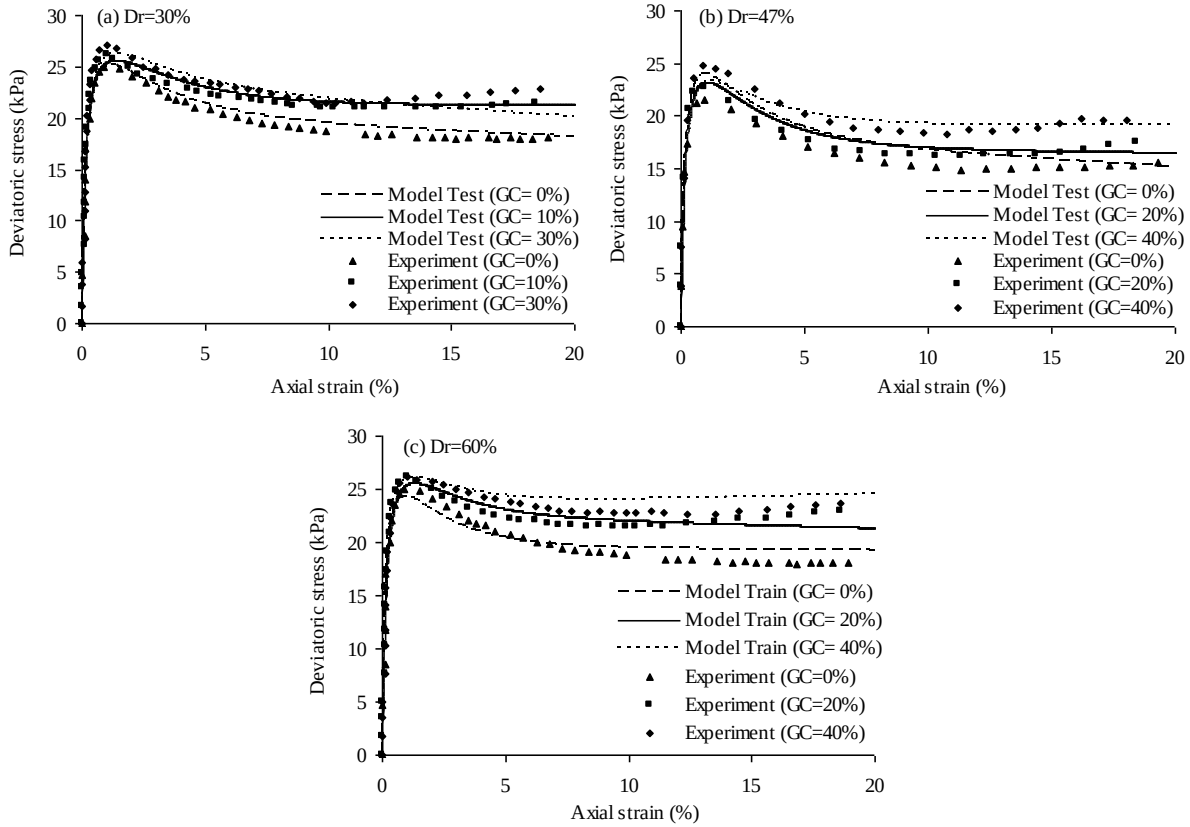

Fig. 5 Comparison of model results with experimental data of Kuenza et al. [8] for deviatoric stress-axial strain curves

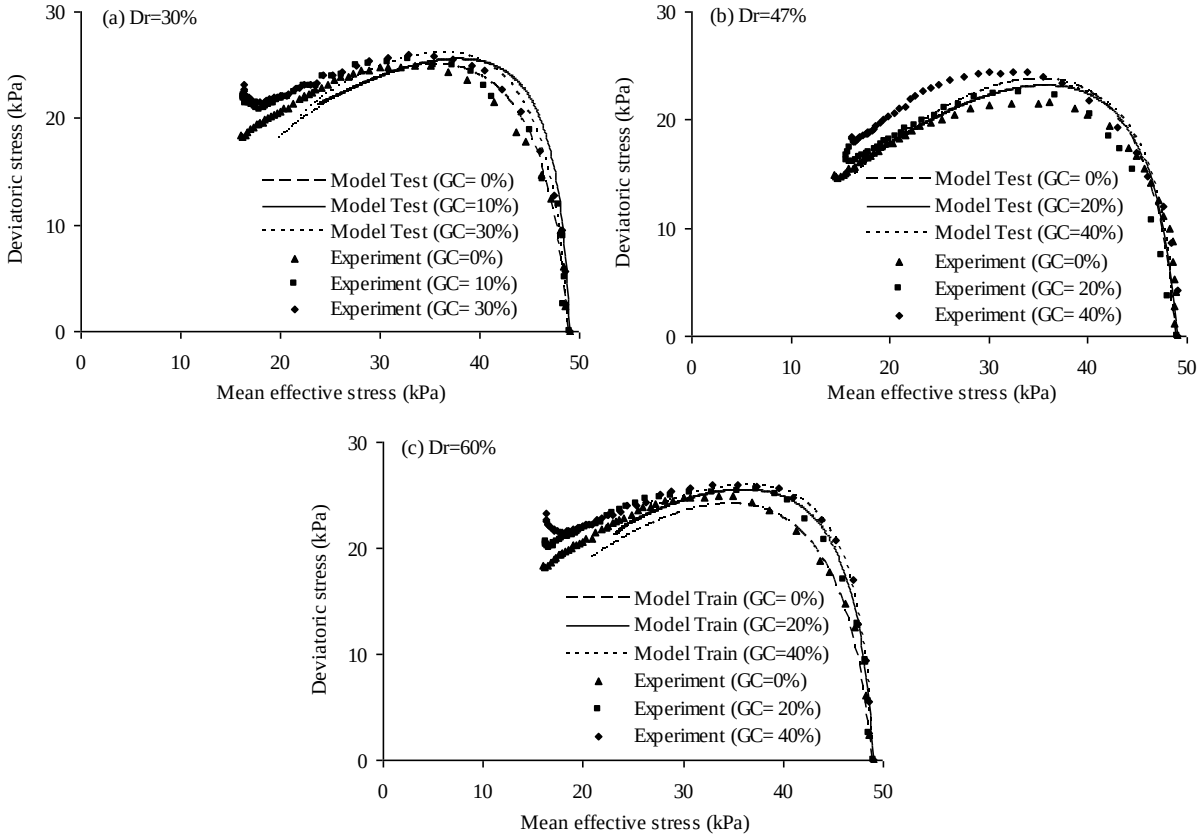

Fig. 6 Comparison of model results with experimental data of Kuenza et al. [8] for deviatoric stress-mean effective stress curves

[DOI: 10.22068/IJCE.13.2.133]

The original GP framework uses Lode angle, θ, for modeling of soil behavior under shear modes other than triaxial one. However, this angle under the torsional shear paths of Kuenza et al. [8] is not similar to that of triaxial test and varies during torsional shear loading. Indeed, it should be noted that the influence of θ is overlooked in present formulation. Although, the results of simulations show that the model is able to predict experimental behavior of torsional shear tests in a good manner.

5.2. Model verification for Verdugo and de la Hoz [13] experimental data

Consolidated drained triaxial tests have been performed on Chilean river sand-gravel mixture under initial confining pressures of 50, 100 and 300 kPa in a relative density of 70%. Table (1) shows physical parameters of tested soil and Table (2) lists the base model parameters for Chilean river sand. Table (4) indicates additional model parameters for sand-gravel mixture with different gravel contents. Test data in two confining stresses of 50 kPa and 100 kPa have been used in model training process and calibration of the parameters. Then, the model is tested for another confinement of 300 kPa. Deviatoric stress-axial strain curves have been depicted in Fig. (7), which show good agreement between experimental data and modeling results.

Table 4 Additional parameters for sand-gravel mixture for tests of Verdugo and de la Hoz [13]

GC (%)	*s*	*a*	*z*	*r*
20	-0.01	0.02	0.025	0.154 (p'_0=50 kPa)
				0.144 (p'_0=100 kPa)
				0.104 (p'_0=300 kPa)
40	-0.01	0.01	0.053	0.216 (p'_0=50 kPa)
				0.206 (p'_0=100 kPa)
				0.166 (p'_0=300 kPa)

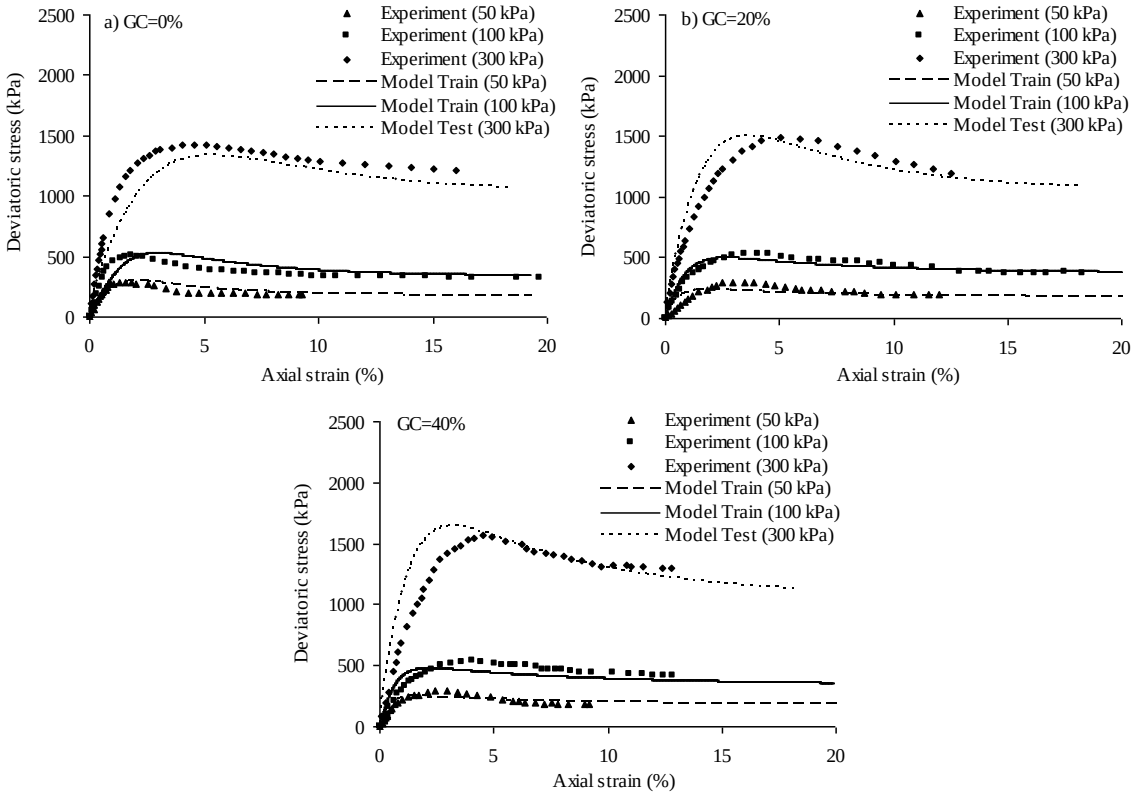

Fig. 7 Comparison of model results with experimental data of Verdugo and de la Hoz [13] for deviatoric stress-axial strain curves

5.3. Model verification for Seif el dine [14] experimental data

Large scale consolidated drained triaxial tests were conducted to investigate the effect of gravel particles on the mechanical behavior of Fontainebleau sand. Gravel particle were added in different volume percentages of 12, 20 and 35 which are equal to weight percentages of 18.46, 29.33 and 47.2 in a constant relative density of 70%.

Table (1) shows the physical parameters of Fontainebleau sand and Table (2) lists 16 parameters of Manzanal et al. base model [36]. Four additional model parameters for sand-gravel mixture have also been depicted in Table (5). Test data for two confining stresses of 50 kPa and 100 kPa are used in calibration process and model training. After that, the model is tested for a confinement of 400 kPa.

[DOI: 10.22068/IJCE.13.2.133]

Figures (8) and (9) compare model results with experimental data for deviatoric stress-axial strain behavior besides void ratio-axial strain ones which shows fairly good consistency between experimental data and simulation results.

Table 5 Additional parameters for sand-gravel mixture in experimental studies of Seif el dine et al. [14]

GC (%)	*s*	*a*	*z*	*r*
				0.145 (p'_0=50 kPa)
18.46	0.02	0.03	0.02	0.135 (p'_0=100 kPa)
				0.075 (p'_0=400 kPa)
				0.20 (p'_0=50 kPa)
29.33	0.01	0.02	0.04	0.19 (p'_0=100 kPa)
				0.13 (p'_0=400 kPa)
				0.235 (p'_0=50 kPa)
47.2	-0.02	0.01	0.06	0.225 (p'_0=100 kPa)
				0.165 (p'_0=400 kPa)

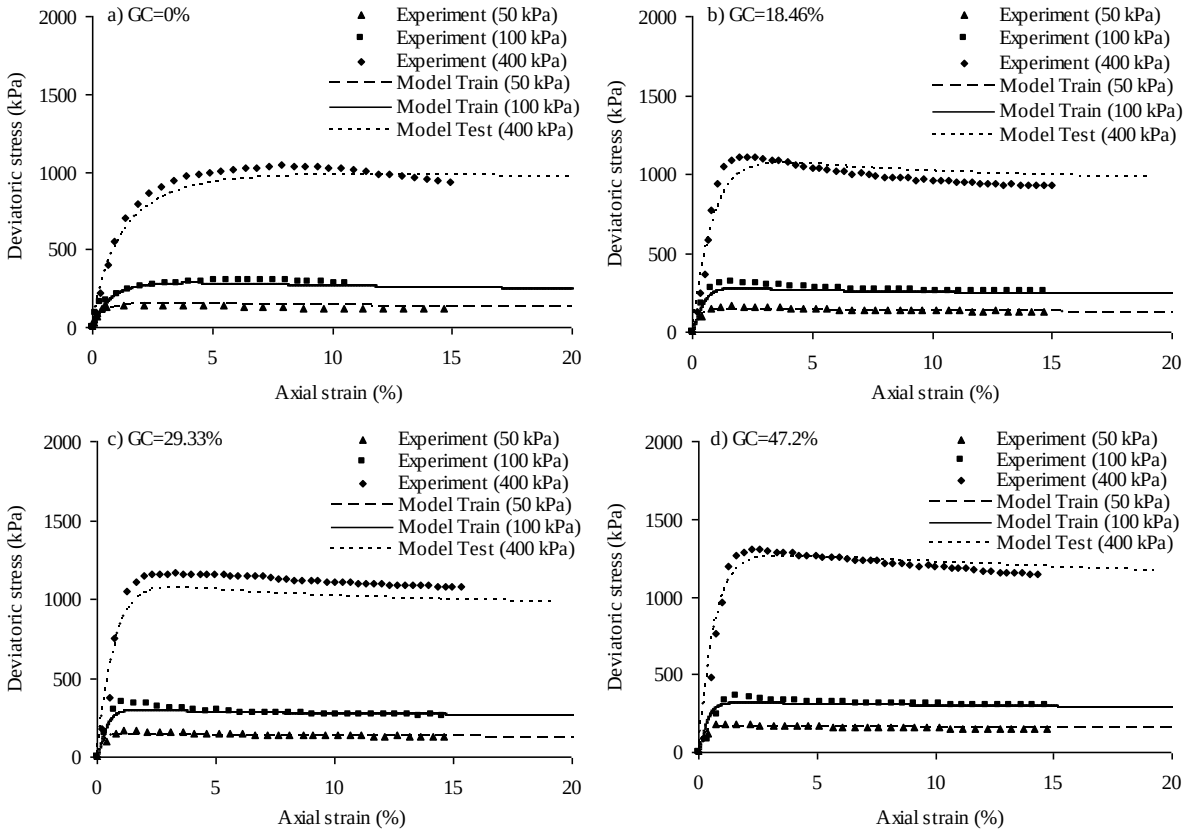

Fig. 8 Comparison of model results with experimental data of Seif el dine et al. [14] for deviatoric stress-axial strain curves

[DOI: 10.22068/IJCE.13.2.133]

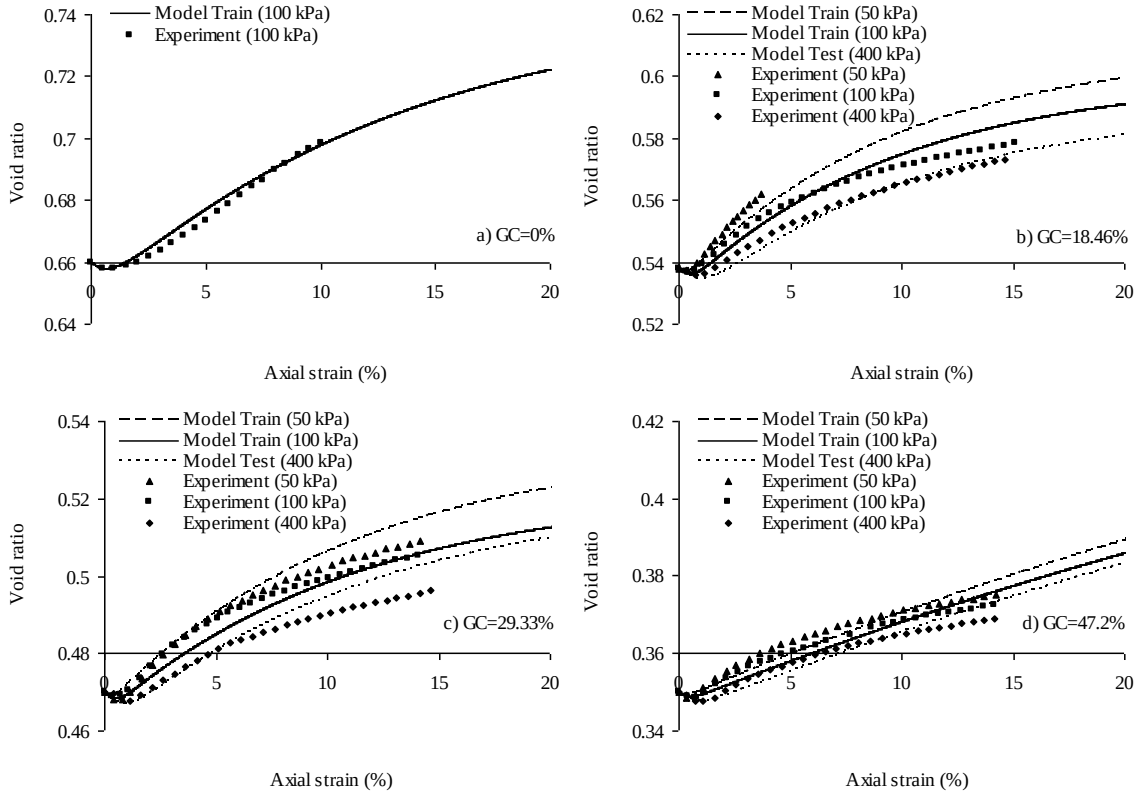

Fig. 9 Comparison of model results with experimental data of Seif el dine et al. [14] for void ratio-axial strain curves

5.4. Model verification for Hamidi et al. [15] experimental data

Using 300mm×300mm×170mm shear box, large scale direct shear tests were performed on Babolsar sand mixed with different percentages of gravel particles under surcharge pressures of 100, 200 and 300 kPa [13]. Table (1) shows physical parameters of Babolsar sand. Base model parameters for Babolsar sand are listed in Table (2). Also Table (6) indicates additional model parameters for sand-gravel mixture. Failure envelopes in shear stress-surcharge pressure ($\tau - \sigma_n$) plane are compared for suggested model and experimental data in Fig. (10) at different gravel contents. Results of comparison are consistent; however, it seems that the slope of the failure envelope which estimates friction angle value slightly decreases with the increase in gravel content.

Table 6 Additional parameters for sand-gravel mixture in experimental studies of Hamidi et al. [15]

GC (%)	*s*	*a*	*z*	*r*
20	0.08	0.03	0.025	0.144 (p'_0=100 kPa)
				0.124 (p'_0=200 kPa)
				0.104 (p'_0=300 kPa)
40	0.04	0.03	0.053	0.206 (p'_0=100 kPa)
				0.186 (p'_0=200 kPa)
				0.166 (p'_0=300 kPa)

[DOI: 10.22068/IJCE.13.2.133]

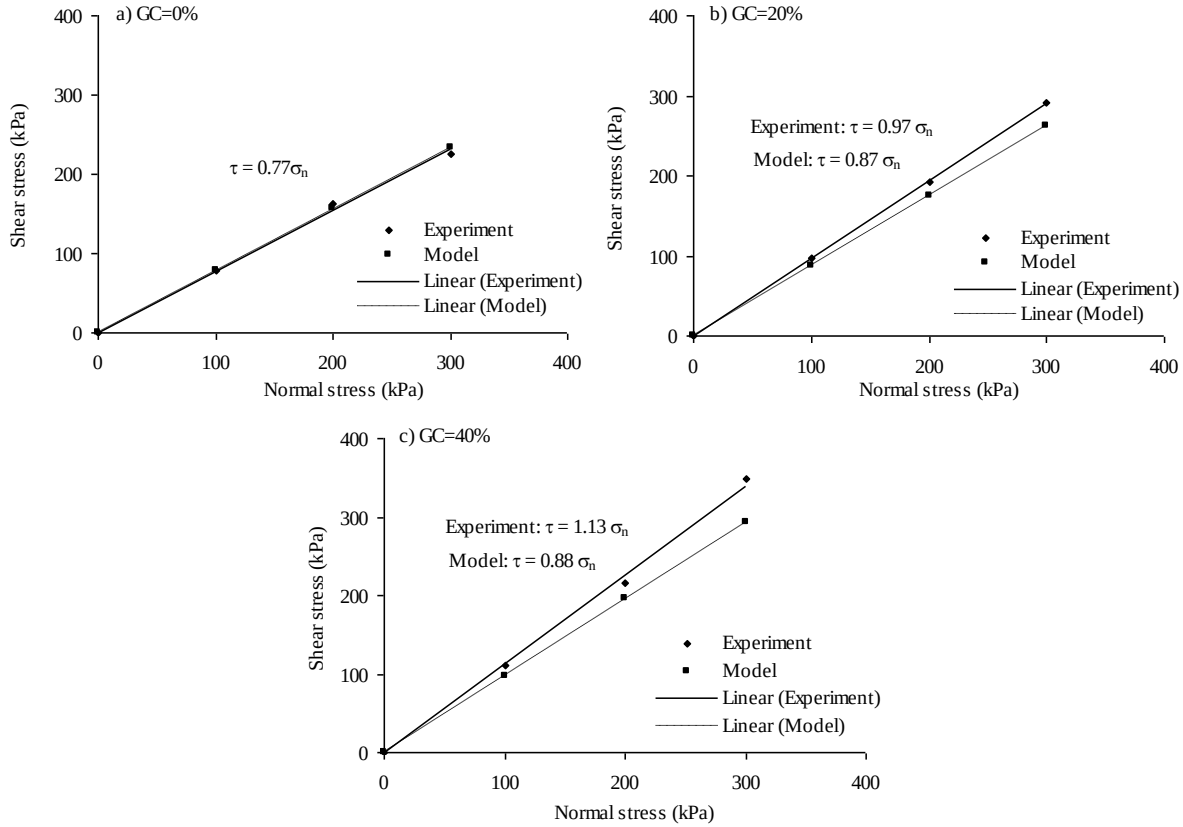

Fig. 10 Comparison of model results with experimental data of Hamidi et al. [15] for the failure envelopes in shear stress-surcharge pressure plane

6. Conclusions

In this paper, a constitutive model is presented for sand-gravel mixtures based on modification of a base critical state model. Manzanal et al. [36] GP model with 16 parameters is used as the base model for sandy soil. In order to consider the effects of gravel content, state parameter, dilation rate and hardening modulus are modified using four new parameters. Verification of the model results is performed using tests in both drained and undrained conditions. Deviatoric stress-axial strain, pore pressure and volumetric strains of the model are compared with experimental results for samples with different gravel contents and relative densities. According to the results of comparison, suggested model is able to predict shear strength characteristics of sand-gravel composite in a good manner. Deviatoric stress-axial strain behavior, volumetric strains in drained condition or pore water pressure in undrained state were correctly simulated. In this regard, the model can be recommended for application in boundary value problems of geotechnical engineering.

Acknowledgments: The authors would like to thank the reviewer for his detailed and constructive comments.

References

[1] Fragaszy RJ, Su J, Siddiqi FH, Ho CL. Modeling strength of sandy gravel, Journal of Geotechnical Engineering, ASCE, 1992, No. 6, Vol. 118, pp. 920-935.

[2] Evans MD, Zhou S. Liquefaction behavior of sand-gravel composites, Journal of Geotechnical Engineering, ASCE, 1995, No. 3, Vol. 121, pp. 287-298.

[3] Kokusho T, Hara T, Hiraoka R. Undrained shear strength of granular soils with different particle gradations, Journal of Geotechnical and Geoenvironmental Engineering, ASCE, 2004, No. 6, Vol. 130, pp. 621-629.

[4] Flora A, Lirer S, Silvestri F. Undrained cyclic resistance of undisturbed gravelly soils, Soil Dynamics and Earthquake Engineering, 2012, Vol. 43, pp. 366-379.

[5] Choi C, Arduino P. Behavioral characteristics of gravelly soils under general cyclic loading conditions, International Conference on Cyclic Behavior of Soils and Liquefaction Phenomena, Bochum, Germany, 2004.

[6] Yagiz S. Brief note on the influence of shape and percentage of gravel on the shear strength of sand and gravel mixture, Bulletin of Engineering Geology and the Environment, 2001, No. 4, Vol. 60, pp. 321-323.

[7] Vallejo LE. Interpretation of the limits in shear strength in binary granular mixtures, Canadian Geotechnical Journal, 2001, No. 5, Vol. 38, pp. 1097-1104.

[8] Kuenza K, Towhata I, Orense RP, Wassan TH. Undrained torsional shear tests on gravelly soils, Landslides, 2004, No. 3, No. 1, pp. 185-194.

[9] Hosseini SM, Haeri SM, Toll DG. Behavior of gravely sand using critical state concepts, Scientia Iranica, 2005, No. 2, Vol. 12, pp. 167-177.

[10] Bolton MD. The strength and dilatancy of sands, Géotechnique, 1986, No. 1, Vol. 36, pp. 65-78.

[11] Simoni A, Houlsby GT. The direct shear strength and dilatancy of sand-gravel mixtures, Geotechnical and Geological Engineering Journal, 2006, No. 3, Vol. 24, pp. 523-549.

[DOI: 10.22068/IJCE.13.2.133]

[12] Verdugo R, De la Hoz K. Caracterización geomecánica de suelos granulares gruesos, Revista Internacional de Desastres Naturales, Accidentes e Infraestructura Civil, 2006, No. 2, Vol. 6, pp. 199-213.
[13] Verdugo R, De la Hoz K. Strength and stiffness of coarse granular soils, Solid Mechanics and Its Applications, 2007, No. 3, Vol. 146, pp. 243-252.
[14] Seif el dine B, Dupla JC, Frank R, Canou J, Kazan Y. Mechanical characterization of matrix coarse-grained soils with a large size triaxial device, Canadian Geotechnical Journal, 2010, No. 4, Vol. 47, pp. 425-438.
[15] Hamidi A, Yazdanjou V, Salimi N. Shear strength characteristics of sand-gravel mixtures, International Journal of Geotechnical Engineering, 2009, No. 1, Vol. 3, pp. 29-38.
[16] Hamidi A, Alizadeh M, Soleimani SN. Effect of particle crushing on shear strength and dilation characteristics of sand-gravel mixtures, International Journal of Civil Engineering, 2009, No. 1, Vol. 7, pp. 61-71.
[17] Hamidi A, Salimi N, Yazdanjou V. Shape and size effects of gravel particles on shear strength characteristics of sandy soils, Scientific Quarterly Journal of GeoSciences, 2011, No. 80, Vol. 20, pp. 189-196.
[18] Hamidi A, Azini E, Masoudi B. Impact of gradation on the shear strength-dilation behavior of well graded sand-gravel mixtures, Scientia Iranica, 2012, No. 3, Vol. 19, pp. 393-402.
[19] Soroush A, Jannatiaghdam R. Behavior of rockfill materials in triaxial compression testing, International Journal of Civil Engineering, 2012, No. 2, Vol. 10, pp. 153-161.
[20] Heidarzadeh M, Mirghasemi AA, Sadr Lahijani SM. Application of cement grouting for stabilization of coarse materials, International Journal of Civil Engineering, 2013, No. 1, Vol. 11, pp. 71-77.
[21] Khan MA. A CBR based study evaluating subgrade strength of flexible pavements having soil flyash interfaces, International Journal of Civil Engineering, 2013, No. 1, Vol. 11, pp. 10-18.
[22] Heshmati AA, Tabibnejad AR, Salehzadeh H, Hashemi Tabatabaei S. Experimental evaluation of collapse deformation behavior of rockfill material, International Journal of Civil Engineering, 2015, No. 2, Vol. 13, pp. 40-53.
[23] Salim W, Indraratna B. A new elastoplastic constitutive model for coarse granular aggregates incorporating particle breakage, Canadian Geotechnical Journal, 2004, No. 4, Vol. 41, pp. 657-671.
[24] Chu BL, Jou YW, Weng MC. A constitutive model for gravelly soils considering shear-induced volumetric deformation, Canadian Geotechnical Journal, 2010, No. 6, Vol. 47, pp. 662-673.
[25] Daouadji A, Hicher PY. An enhanced constitutive model for crushable granular materials, International Journal for Numerical and Analytical Methods in Geomechanics, 2010, No. 6, Vol. 34, pp. 555-580.
[26] Xiao Y, Liu HL, Zhu JG. A 3D bounding surface model for rockfill materials, Science China Technological Sciences, 2011, No. 11, Vol. 54, pp. 2904-2915.
[27] Pastor M, Zienkiewicz OC, Chan AHC. Generalized plasticity and the modeling of soil behavior, International Journal for Numerical and Analytical Methods in Geomechanics, 1990, No. 3, Vol. 14, pp. 151-190.
[28] Zienkiewics OC, Mroz Z. Generalized plasticity formulation and application to geomechanics, Mechanics of Engineering Materials, 1984, No. 2, Vol. 44, pp. 655-679.
[29] Ling HI, Liu H. Pressure level dependency and densification behavior of sand through the generalized plasticity model, Journal of Engineering Mechanics, 2003, No. 8, Vol. 129, pp. 851-860.
[30] Ling HI, Yang S. A unified sand model based on critical state and generalized plasticity, Journal of Engineering Mechanics, 2006, No. 12, Vol. 132, pp. 1380-1391.
[31] Santaguliana R, Schrefler BA. Enhancing the Bolzon-Schrefler-Zienkiewicz constitutive model for partially saturated soil, Transport in Porous Media, 2006, Vol. 65, pp. 1-30.
[32] Lashkari A, Latifi M. A constitutive model for sand liquefaction under continuous rotation of principal stress axes, Mechanics Research Communications, 2009, Vol. 36, pp. 215-223.
[33] Liu H, Ling HI. Constitutive description of interface behavior including cyclic loading and particle breakage within the framework of critical state soil mechanics, International Journal for Numerical and Analytical Methods in Geomechanics, 2008, No. 12, Vol. 32, pp. 1495-1514.
[34] Lashkari A. Modeling of sand-structure interfaces under rotational shear, Mechanics Research Communications, 2010, Vol. 37, pp. 32-37.
[35] Weng MC, Ling HI. Modeling the behavior of sandstone based on generalized plasticity concept, International Journal for Numerical and Analytical Methods in Geomechanics, 2013, Vol. 37, pp. 2154-2169.
[36] Manzanal D, Merodo JAF, Pastor M. Generalized plasticity state parameter-based model for saturated and unsaturated soils: Saturated state, International Journal for Numerical and Analytical Methods in Geomechanics, 2011, No. 12, Vol. 35, pp. 1347-1362.
[37] Been K, Jefferies MG. A state parameter for sands, Geotechnique, 1985, No. 2, Vol. 35, pp. 99-112.
[38] Li XS, Wang Y. Linear representation of steady-state line for sand, Journal of Geotechnical and Geoenvironmental Engineering, 1998, No. 12, Vol. 124, pp. 1215-1217.

[DOI: 10.22068/IJCE.13.2.133]